DEVELOPMENT OF A SUBSCALE FLIGHT TESTING PLATFORM FOR A GENERIC FUTURE FIGHTER

Amadori, K.*, Jouannet, C.*, Berry, P.**
***Linköping University**
****Saab AB**

Keywords: *subscale, demonstrator, flight testing*

Abstract

One branch of the current research in aircraft design at Linköping University is focused on fast concept evaluation in early design stages. This covers multidisciplinary optimization using tools of different level of complexity and low-cost subscale flight testing. In some cases a flight test will provide more answers than several computations ever could. In order to achieve this goal a methodology is required to allow fast creation of subscale flying concepts and to obtain as much reliable information as possible from the tests. The methodology is currently being developed. One important part of it is the scaling methodology and the imposed requirements on manufacturing. The present paper presents the latest subscale demonstrator from Linköping University that has been built as part of the study initiated by the Swedish Material Board on a Generic Future Fighter aircraft.

1 Background

In 2006 a research study from the Swedish Material Board (FMV) was initiated. The study concerned aeronautical design and integration of a Generic Future Fighter (GFF) with stealth capabilities, super-cruise and long range. The study involved the following parties: Saab AB, the Swedish Defense Research Agency (FOI), Volvo Aero, Linköping University and the Royal Institute of Technology (KTH).
The specification of the GFF asked for:

- Multirole
- Stealth
- Internal payload bays
- Super-cruise
- Integration of future sensors and system architecture
- Studies of a new engine
- Scaled demonstrator

The concept for the GFF was developed with support by FOI during 2006.
The aircraft has three internal payload bays in the fuselage. Two centrally placed for heavier payload, located close to the center of gravity and one forward bay for lighter payload (Fig. 1).

Fig. 1 General view of the Generic Future Fighter (GFF)

The basic configuration is a canard, i.e. a stealthy development of the Gripen system. The aircraft has canted fixed fins by stealth reasons, which also work as control and trim surfaces in plan view together with the all moveable canards.

Table 1 gives the basic dimensions and estimated weights.
Fig. 2 and Fig. 3 show the basic structural layout and placement of some systems and fuel.

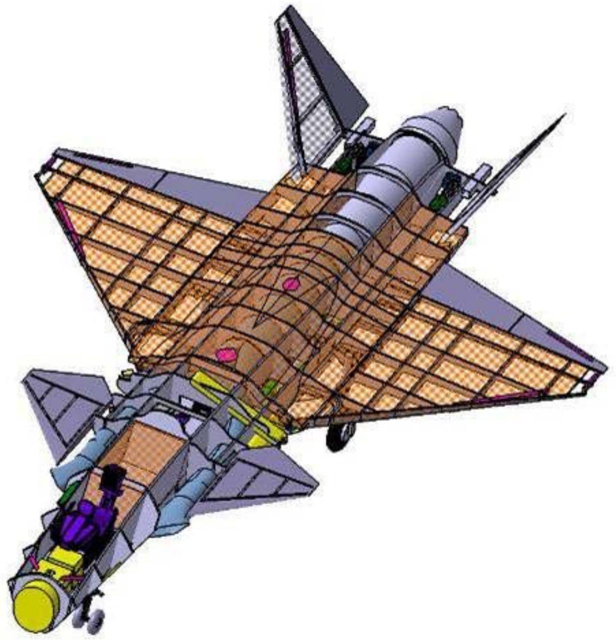

Fig. 2 Structure and general layout, top view

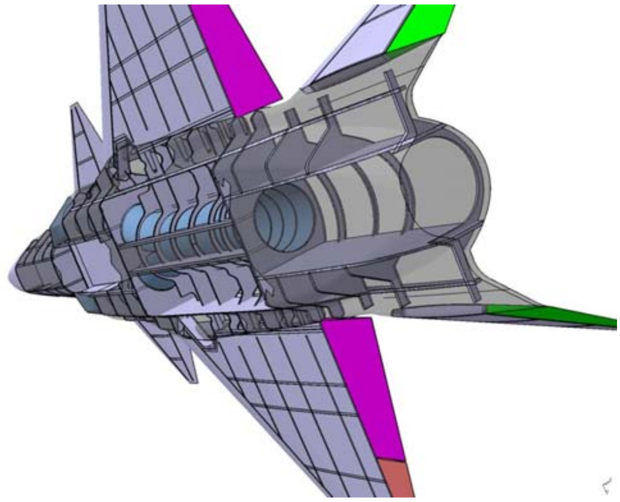

Fig. 3 Structure and general layout, view from below

Length	[m]	17
Height	[m]	4
Span	[m]	10,5
Wing Area	[m^2]	
OEW	[kg]	10000
Design Weight	[kg]	15400
Internal Fuel	[kg]	6200
MTOW	[kg]	23500
New Engine with AB	[kN]	170

Table 1 GFF's main characteristics

The location of the fin relative to the vortices created by the sharp edges of the forebody and/or canard at high angles of attack caused some concern at early design stages. This has been a major problem in the past on similar aircraft configurations (like the Boeing F/A-18 Hornet and the Lockheed F-22 Raptor) with potential flutter and/or fatigue problems, requiring structural modifications and hence a heavier structure than anticipated. FOI were asked to investigate this problem in their CFD studies and discovered that the matter could turn up to be a serious issue also for the GFF (Fig. 4).
Alternative configurations were also considered to examine if there might be a design solution to the potential problem (Fig. 5).

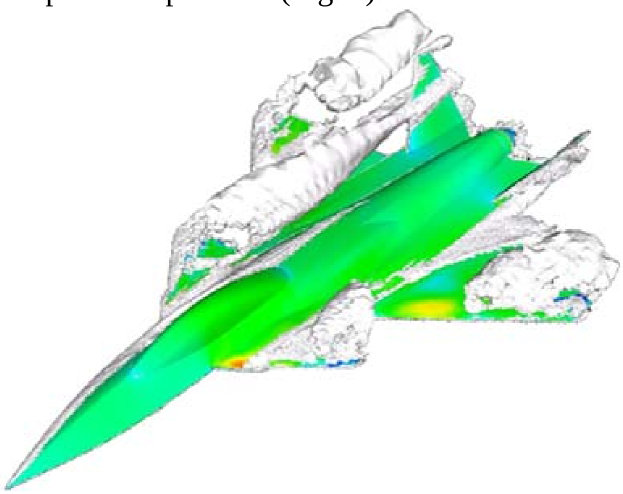

Fig. 4 FOI CFD studies. Notice the vortices hitting the fins

Fig. 5 Alternative design with winglets

The alternative configuration in Fig. 5 has canted winglets replacing the fins. This requires a more swept and cranked wing to increase the moment arm. The good effect of this solution was that the area distribution at the rear end became considerably better than in the previous concept, but flutter in the wing due to the winglets was raised as a new even worse potential problem. Therefore it was decided to keep the original layout and try to live with the situation.

FOI studied also the flow in open weapon bays on release of the weapons and could list some problem areas there [14].

Volvo Aero studied a new engine while Linköping University designed, built and flew a down-scaled demonstrator that will be described in detail in this paper.

The study finished in 2009.

2 Introduction

Subscale flight testing is a means of allowing the design team to evaluate the flight characteristics prior to building a full-scale prototype. It also permits to investigate extreme, high-risk portions of the flight envelope without risking expensive prototype air vehicles. Another field of application that is suggested in this work is to use subscale flight vehicles as a means of evaluating, demonstrating and comparing high-risk platforms and technologies without the prohibitive expense of a full-scale vehicle.

There are several recent examples of this kind of testing strategies. The NASA funded McDonnell Douglas X-36 [2],[3], the Rockwell HiMAT [4], the Saab UCAV [5], the NASA X-43A-LS [6] and the proposed Gulfstream Quiet Supersonic Jet [7] can be listed as examples. In all cases the configurations are highly unconventional and thus there is a desire to demonstrate the configuration's feasibility without the cost or risk of a manned, full-scale vehicle.

The testing of subscale flight models is not new. Particularly for dangerous tests, such as high angle-of-attack or to study departure modes, where flying subscale aircraft allow to avoid the restrictions imposed by a rigid connection that is necessary during wind tunnel trials.

Spin models for updraft wind tunnels have been a standard practice since the 1940s and remotely controlled drop models from helicopters have often been used to complement spin tunnel testing (a typical example being the Saab Viggen test program [8]). Among the more unique examples of subscale testing the Saab Draken could be remembered. In order to test the aerodynamics of the double delta wing - in addition to numerous drop models and models fixed to the nose of rockets for high speed tests - a subscale manned aircraft (the Saab 210 "*Lilldraken*"), with a planform similar to the proposed aircraft, was tested prior to full-scale development. Free flight models have also been built for conventional wind tunnels, such as the NASA Langley Free Flight Facility [9]. For fighter configurations, drop models have also been widely used; recent examples being the X-31 [10] and F/A-18E/F. Subscale drop models of space vehicles such as the Lockheed Martin X-38 and Japanese HOPE-X [11] have also been undertaken. Recently the usage of subscale flight testing has been extend to civil aircraft, such as within the NASA Airstar research program, where scale models are used to explore a larger flight envelope for a civil transport aircraft. Hence it is possible to evaluate the different risks that can be encountered during take-off, landing or under heavy gusts. For blended wing body concepts, the X-48 program from Boeing and NASA is currently using a scaled model to demonstrate the concept and obtain more data without going to full-scale.

3 Scaling Methods

Different scaling methods can be employed. Key scaling similarity conditions that must be met in order to achieve full similarity are:

- Geometric similarity
- Aerodynamics
- Reynolds number (inertia-to-viscous forces ratio)
- Mach number (inertia-to-pressure force ratio)
- Inertial scaling
- Froude scaling

Note that the scaling problem becomes even more difficult when aeroelastic effects need to be considered; they are however neglected for the purposes of this discussion.

Significant discussions exist as to what degree, and whether, all of these parameters need to be closely matched to ensure similar characteristics between the subscale and full-scale vehicles. They are more than likely dependent on the vehicle itself and the characteristics which are being sought. For example, departures such as spin, require correct inertial scaling whereas take-off and landing performance tests are more dependent on aerodynamic and thrust matching. Detailed information on the different scaling methods can be found in a previously published article by the authors [15] and in the review paper of Wolowicz et al. [12].

4 Scaled Model

The demonstrator was scaled down to 13% of the full–scale aircraft. The factors influencing the choice were mainly handling and transportability. However, weight estimation and availability of jet engines were also carefully considered. As it will be explained soon, the chosen engine was a JetCat P160, capable of delivering 160 N of thrust [13]. As design revisions suggested and initial water tunnel testing and CFD analyses proved, the aircraft geometrical layout pushes at high angles of attack vortices that invest the fins (see section 8 “Water Tunnel Testing” for more details). From a construction stand point, this meant that the aft section of the aircraft required the highest possible rigidity and stiffness in order to prevent catastrophic events to incur during flight. Hence a series of measures were taken to achieve maximum robustness (see section 6 “Manufacturing”).

Another important issue was whether to install the engine as far back as possible or close to the center of gravity. The latter was finally chosen, as will be explained in section 7 “Engine and Fuel System Installation”.

It should also be pointed out that great care was dedicated to the landing gear installation so that the exact attitude and footprint as the full-scale aircraft would be maintained. Fig. 6 shows a CAD representation of the demonstrator with all main components.

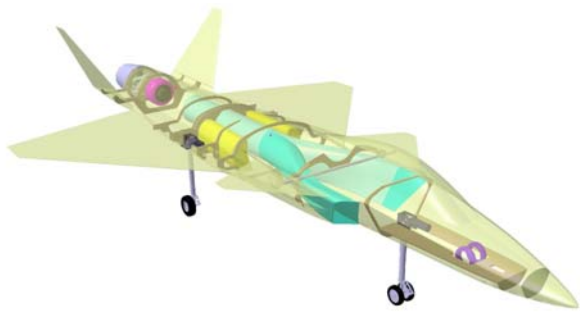

Fig. 6 Complete CAD model of the demonstrator

4.1 Scaling Method

Ideal scenario would have been to dynamically scale and design the demonstrator aircraft so that it would get the same dynamic properties as the full-scale aircraft. This does not mean that the demonstrator should be able to maneuver exactly like the full-scale aircraft. It means that the demonstrator should have the same response according to scale. However in the presented case it has not been possible to realize dynamic scaling.

In this project Froude scaling is used, originating from the similarity parameter Froude number N_{Fr}:

$$N_{Fr} = \frac{V^2}{\ell \cdot g} \quad (1)$$

where V is the speed, g is the gravitational acceleration and ℓ is a characteristic length. The essence of the method is that it compensates for inertial and gravitational effect, thus assuming that two objects flying at different speed, altitude, etc. have the same Froude number. From that conversion factors, a wide spectrum of quantities can be derived: forces, moments, Reynolds number, angular rates, etc. For instance, if a characteristic length (ℓ) is to be scaled, the following relation can be used:

$$\frac{\ell_M}{\ell_A} = n \quad \rightarrow \ell_M = n \cdot \ell_A \qquad (2)$$

where the subscript *M* denotes *model*, subscript *A* denotes *actual aircraft*.
The weight was calculated from the following equation:

$$W_M = k^3 \cdot W_{fs} \cdot \frac{d_M}{d_{fs}} \qquad (3)$$

It can be seen from the equation above that the model weight is determined from full-scale aircraft weight and altitude, or conversely, a given model weight can represent different combinations of aircraft weight and altitude.
Dimensions are decided by the following equation:

$$l_M = k \cdot l_{FS} \qquad (4)$$

where the subscript *FS* denotes *full-scale*.
From scaling and similitude requirements, a subscale model must respond faster than a full scale model by a factor of $\sqrt{k}$. Mass moments of inertia of the model are related to the inertias of the full-scale aircraft by a factor of k^5.
Different scaling factors were considered; if dynamically scaling was to be achieved a scale factor of 10 to 11% should have been chosen with regard to weight, but due to overall geometrical considerations the demonstrator resulted hard to reduce to such a scale. Therefore the demonstrator was not to dynamically scaled, but only scaled according to aerodynamic similarities. The size was set to 13% due manufacturing and available of RC component. Another difficult issue was that no exact data on the inertia matrix was available from the full-scale study. Since the full-scale aircraft is an "unstable" configuration, and due to the fact that the demonstrator will be remotely controlled, the demonstrator has to be a stable aircraft. Hence the possibilities of a dynamically scaled model are reduced even more.

Scale	Size [mm]	Wing Span [mm]	Weight [kg]	Design Weight [kg]
1,00	17000	10500	23500	15400
0,17	2890	1785	115,456	75,660
0,16	2720	1680	96,256	63,078
0,15	2550	1575	79,313	51,975
0,14	2380	1470	64,484	42,258
0,13	2210	1365	51,630	33,834
0,12	2040	1260	40,608	26,611
0,11	1870	1155	31,279	20,497
0,10	1700	1050	23,500	15,400

Table 2 GFF's main dimensions as function of scaling factor

5 Flight Test Equipment

The rapid development of low-cost and miniaturized electronics has been a key enabling technology to the development of subscale vehicles. The objective of this part of the work has been to construct an instrumentation package consisting of both the ground and airborne package. The basic system layout used in this work is given in Fig. 7. The control of the airplane is realized by a RC transmitter, while the standard receiver has been replaced by a redundant system to minimize transmission looses. The usage of a RC radio link for the control was to simplify the system in a first stage. The system is described in full detail by Lundström and Staack [20].

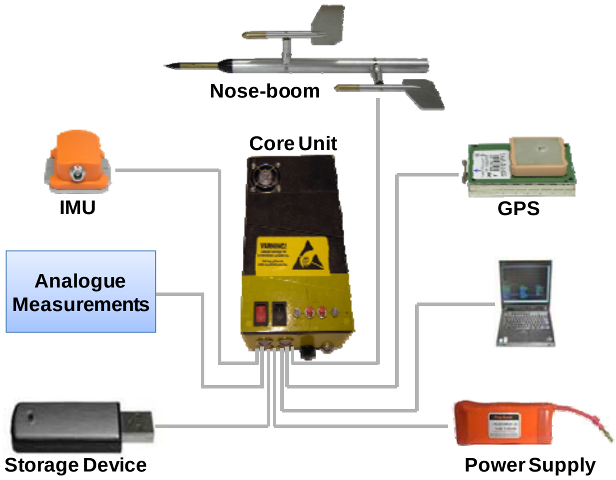

Fig. 7 The flight test equipment

6 Manufacturing

The subscale model aircraft is realized in composite materials with the internal structural elements of the fuselage made of plywood and carbon-fiber. The composite was realized as a sandwich of two glass-fiber layers and one Herex™ sheet, cured in vacuum bags. The moulds were milled from RenShape™ 5460 blocks directly from the outer mould-line of the aircraft defined in CATIA V5. Using the CAD model of the scaled aircraft, the moulds were carefully designed. Simulation of manufacturing of the fuselage halves showed early on that, due to the particular shape of the aircraft, undercuts in the air intake region could not be avoided. Therefore the upper fuselage mould was designed with removable parts, as shown in Fig. 8. The wings are instead built with a different technique. A core was cut from high density foam and covered with a sandwich of balsa and glass-fiber. Two 14 mm carbon-fiber rods were used as load-carrying wing beams.

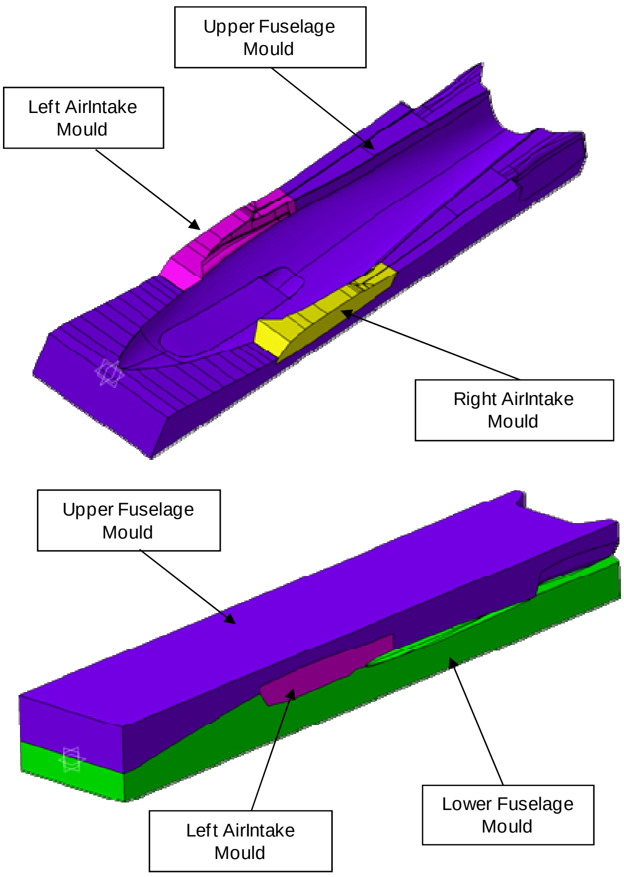

Fig. 8 Moulds for the fuselage were designed in CATIA V5

Fig. 9 The scaled GFF aircraft

A similar manufacturing process was employed for both canards and vertical tails. But, in the fins, carbon-fiber was employed instead glass-fiber. The reason is to enhance the tails' stiffness (as previously anticipated) as one of the measures taken to counteract the negative effects of the vortices hitting the fins. Other actions taken were:

- solid carbon-fiber rod was used as load carrying beam for the vertical tails;
- fuselage frames were cut out of solid pre-cured carbon-fiber plates instead of plywood as in the rest of the fuselage.

Moreover two pairs of fins were manufactured: one pair with moving rudders and another without. The reason was to be able to carry out initial flights with non-moving tails to reduce risks for flutter. The tails with moving rudders are planned to be employed only after initial flight tests have evaluated structural rigidity, vortex intensity and flutter risk.

7 Engine and Fuel System Installation

For the demonstrator a JetCat P160 engine was chosen. The engine is capable of producing up to 160 N of thrust and is a reliable engine used in hobby radio controlled aircraft. Even though not required by the Saab or FOI, the group decided to install also a thrust-vectoring exhaust pipe that enables to deflect the jet stream ±15 degrees both on the horizontal and vertical plane.

As previously anticipated, the biggest issue concerning the engine installation was where to place the engine in the fuselage. Two variants were considered and weighted against each other. In the first one the engine was to be installed at the very end of the fuselage, while in the second it would have been placed in the middle of the aircraft. The main advantages with the first variant (also shown in Fig. 6) were:

- safety distance between fuel tanks and engine;
- no need for a heat-resistant exhaust tube, which was predicted to weight around 600 g;
- closeness between engine exhaust and the thrust-vectoring exhaust pipe;
- simplified engine installation and maintenance.

This solution presented though the disadvantage of placing one of the heaviest components far back in the aircraft. By installing the engine in the middle of the fuselage it was possible to save up to 800 g on total empty weight. Inertial characteristics were also favored by the latter solution. Hence the decision was taken to install the engine in a central position.
The fuel system consists of two main tanks slightly larger than two liters, connected in parallel to the engine feed via a hopper tank and a so-called bubble trap that blocks any air bubble within the fuel from being fed to the engine. Fig. 10 shows schematically how all components are connected.

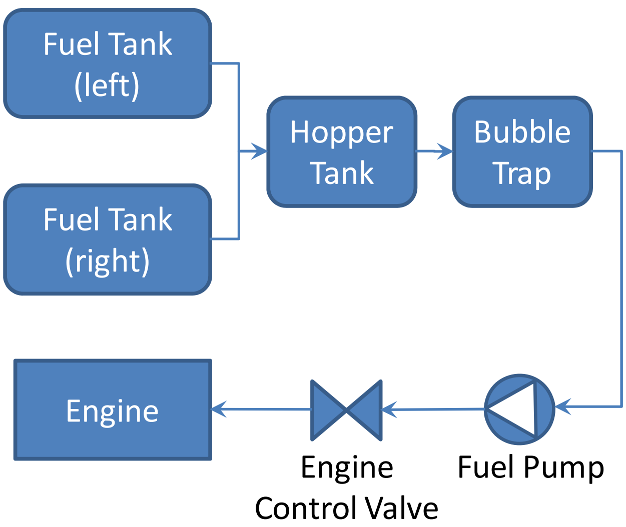

Fig. 10 Scheme of the installed fuel system

Attention was paid in order to guarantee that the main tanks would be positioned close to the center of gravity. Due to the engine position, shields were placed between the engine and the fuel system components.

8 Water Tunnel Testing

Water tunnels have been extensively used for flow visualization of aircraft aerodynamics for at least forty years. Among the purported advantages of water tunnels are lower cost and more readily obtainable flow visualization of the separated (vortex-dominated) flows. In comparison to the wind tunnel, in a water tunnel the flow is entirely laminar and thus the tracer does not disperse into the fluid to the same extent as in turbulent flow. As such, dye tracers (typically food dye) are widely used because of their cost, safety and reliability.
There is however a major concern with the use of water tunnel facilities for the study of aircraft aerodynamics. Reynolds number scaling is far from achieved in such tests, typically being of three to four orders of magnitude smaller than full-scale. Table 3 gives a typical indication of the test conditions for a high angle-of-attack test in water and wind tunnels compared to flight. This difference in Reynolds number similarity means that the boundary layer will typically be five to six times thicker in the water tunnel than wind tunnel. Furthermore, strongly Reynolds number dependent flow features, such as transition and separation, will be entirely misrepresented.
As such, it is unreasonable to expect water tunnel testing to provide useful information where the flow topology is dominated by such Reynolds number dependent flow features.

Facility	Re	M	Q(Pa)
Water tunnel	$O(10^4)$	$O(10^{-5})$	5 - 50
Wind tunnel	$O(10^5 - 10^6)$	0.03 - 0.6	60 - 6000
Flight	$O(10^7)$	0.2 - 0.8	$O(10^3 - 10^4)$

Table 3 Typical test conditions in aeronautical facilities

However, for detached flows where vortices are dominant the situation is somewhat different. Vortex breakdown has been extensively investigated experimentally, theoretically and more recently computationally and is a subject of much ongoing research. It is of interest because of the rapid change in local pressures that are introduced, particularly as regards stall and local buffeting, and also because of the time delay and nonlinearities introduced.

8.1 Experimental Setup

The water tunnel used in the present study is an Eidetics model 1520 tunnel with a test section of 38 x 51 x 152 cm. The tunnel has a maximum test section velocity of around 30 cm/s and turbulence level below 1.0%. The model was supported on a C-strut mechanism capable of an angle-of-attack range from -15° to +80° and sideslip of ±20 ° and roll of 360°. The water tunnel has just been upgrade with the free roll angle in order to allow any type of motion and two cameras that follow the test object path in order to obtain the best possible pictures and movies.

8.2 Flow Visualization

Food dye was used as the flow tracer. Metal tubing of 0.5 mm outer diameter were located flush on the forebody at a transition point between round and shined forebody, at the canard apex and at the wing apex. Experience indicated that the optimum water velocity for flow visualization was around 10 to 14 cm/s. In order to capture the flow unsteadiness a digital video camera was used to acquire the images. The frames were subsequently extracted from this video and analyzed with the aid of a MATLAB-based code. Identification of the vortex trajectories and breakdown was achieved using the mouse to identify a set number of points; it was felt this procedure was more accurate than image recognition and more flexible as at times the vortices were difficult to detect.
The position of the kink in the vortex core was used as the reference point for vortex breakdown.
Modern fighters' configurations with shined forebody and Leading Edge Extensions have shown flow field dominated by vortices. The vortices over such configurations are well known to contribute to excess of lift. The breakdown of those vortices has been the primary cause of severe tail buffeting on the F/A-18 E/F [16],[17],[19], and similar behavior has been observed on the F-22 [18]. Due to the GFF's configuration similarities, the water tunnel experiment was set up to investigate the vortex breakdown behavior and its relative location to the fin.

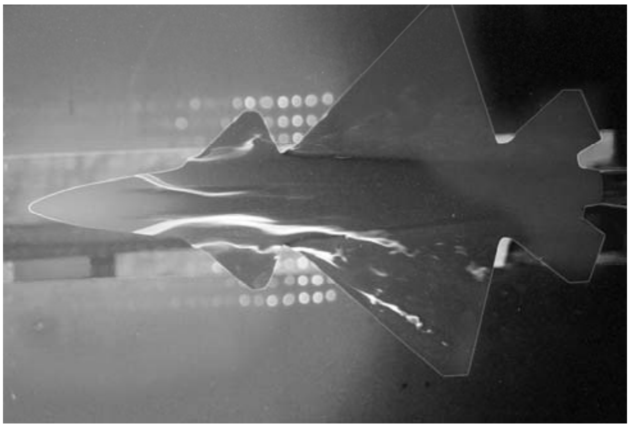

Fig. 11 Flow field over GFF

The water tunnel investigation indicates that for some angles of attack the wake behind the vortex breakdown due to the forebody/canard impinges on the tail surfaces as suspected, see Fig. 11.

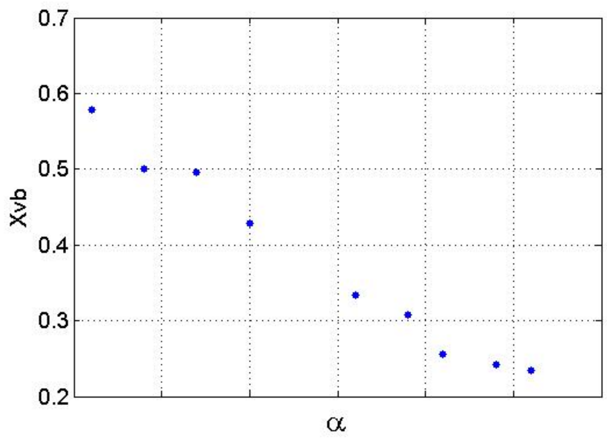

Fig. 12 Wing vortex breakdown location (Xvb) relative to the angle of attack (α)

The wing vortex breakdown location moves toward the apex as angle of attack is increased, Fig. 12. The spread angle for the vortex over the wing is fairly constant at all angles of attack.
In figure Fig. 13 a strong interaction between the forebody vortex and the vortex emanating from the canard can be observed. No clear

coupling between the wing vortex and the other vortices were observed.

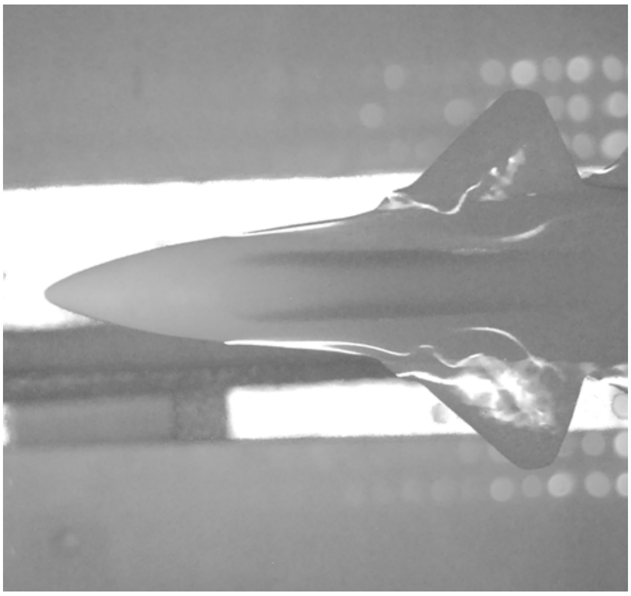

Fig. 13 Interaction between forebody vortex and canard vortex

9 Conclusions and Future Work

The paper presents the latest subscale demonstrator that has been designed and manufactured at Linköping University. The aircraft is a scaled down version of the Generic Future Fighter (GFF) that incorporates the results from a research initiated by the Swedish Material Board (FMV) in 2006. The study concerned aeronautical design and integration of an aircraft with stealth capabilities, super-cruise and long range.

After a successful maiden flight, the flight testing is about to begin and will continue long after summer and fall 2010. Data logging equipment has also been designed and installed in the vehicle in order to collect different parameters, such as position, speed, accelerations, angular rates, engine and servo signals…

Flight testing will also allow the visualization of the flow field in different conditions. Wood yarns and possibly smoke generators will be adopted for the task.

Water tunnel and CFD analyses have also been carried out and indicate potential problems due to vortex brake-down at higher angles of attack that seem to invest the fins. Further and deeper studies and tests will be performed to investigate the matter and to try different solutions. The demonstrator will be flown to specifically explore the effects of the vortices on the fins and the risk for potential problems.

10 Acknowledgement

The authors would like to express their gratitude for all precious contributions to David Lundström and Ingo Staack. Special thanks also to FMV for founding the project and Kunt Överbrö at Saab AB for making all this possible.

References

[1] Smith J, Jones B and Brown J. *The title of the book*. 1st edition, Publisher, 2001.

[2] Dornheim, M.A., "*McDonnell Douglas Rolls Out X-36*", Aviation Week & Space Technology, 144(13), 1996.

[3] Walker, L.A., "*Flight Testing the X-36 - The Test Pilot's Perspective*", Technical Report NASA CR-198058, 1997.

[4] Deets, D.A., DeAngelis, V.M., Lux, D.P., "*Himat Flight Program: Test Results And Program Assesment Overview*", Technical Report NASA TM-86725, 1986.

[5] "*Saab Tests Subscale UCAV Concept*". Flight International, 162, 2002.

[6] Gibson, C.S., Neidhoefer, J.C., Cooper, S.M., Carlton, L., Cox, C.J., "*Development And Flight Test Of The X-43a-Ls Hypersonic Configuration UAV*", AIAA Paper 2002-3462, 2002.

[7] Warwick, G., "*Gulfstream Unveils Concepts For Supersonic Business Aircraft*", Flight International, 158(4751), 2000.

[8] Henriksson, K.E., "*Spin Testing the Viggen Aircraft. Technical Report*", Society of Experimental Test Pilots, 1974.

[9] Hahne, D.E., Wendel, T.R., Boland, J.R., "*Wind-Tunnel Free-Flight Investigation of a Supersonic Persistence Fighter*", Technical Report NASA TP-3258, 1993.

[10] Klein, V., Noderer, K.D., "*Aerodynamic Parameters Of The X-31 Drop Model Estimated From Flight-Data at High Angles Of Attack*", AIAA-1992-4357, 1992.

[11] Yanagihara, M., Miyazawa, Y., Alimoto, T., Sagisaka, M., Cretenet, J.C., Venel, S., "*HOPE-X High Speed Flight Demonstration Program Phase II*", AIAA Paper 2001-1805, 2001.

[12] Wolowicz, C.H., Bowman Jr., J.S., Gilbert, W.P., "*Similitude Requirements and Scaling Relationships*

as Applied to Model Testing", Technical Report NASA TP-1435, 1979.

[13] JetCat USA homepage (June 13th, 2010), http://www.jetcatusa.com/p160.html

[14] Berglind, T., Peng, S-H., Tysell, L., "*FOT25: Studies of Embedded Weapon Bays – Summary Report*", FOI-R—2775—SE Technical Report

[15] Jouannet, C., Lundström, D., Amadori, K., Berry, P., "*Design of a Very Light Jet and a Dynamically Scaled Demonstrator*", AIAA-2008-137, 46th AIAA Aerospace Sciences Meeting and Exhibit, Jan. 2008, Reno, NV, USA

[16] Moses, Robert W. and Huttsell, Lawrence J.: "*Fin Buffeting Features of an Early F-22 Model*" 41st AIAA/ASME/ASCE/AHS/ASC Structures, Structural Dynamics, and Materials Conference and Exhibit, Atlanta, Georgia, AIAA 2000-1695, April 3-6, 2000, pp. 10.

[17] Erickson, G. E., Hall, R. M. Banks, D. W., et.al, "*Experimental Investigation of the F/A-18 Vortex Flows At Subsonic Trought Transonic Speeds*", AIAA 89-2222.

[18] Robert W. M., "*Nasa Langley Research Center's Contributions to International Active Buffeting Alleviation Programs*" Paper presented at the RTO AVT Specialists' Meeting on "Structural Aspects of Flexible Aircraf Control", Ottawa, Canada, 18-20 October 1999, and published in RTO MP-36.

[19] Anthony S. P. and Robert W. M., "*A Method to Analyze Tail Buffet Loads of Aircraft*", Paper presented at the RTO AVT Symposium on "Flow-Induced Unsteady Loads and the Impact on Military Applications," Budapest, Hungary, 25-29th April 2005 and published in RTO-AVT-123/RSY

[20] Lundström D., Staack, I., "*Subscale Flight Testing at Linköpings University*", ICAS 2010, Sept. 19th-23rd 2010, Nice France.

Copyright Statement